Materials Transactions, Vol. 47, No. 11 (2006) pp. 2835 to 2841

Three Temperature Model for Nonequilibrium Energy Transfer in Semiconductor Films Irradiated with Short Pulse Lasers

Seong Hyuk Lee, Hyung Sub Sim, Junghee Lee, Jong Min Kim and Young Eui Shin*

School of Mechanical Engineering, Chung-Ang University, Seoul, Korea

This article investigates numerically carrier-phonon interaction and nonequilibrium energy transfer in direct and indirect bandgap semiconductors during sub-picosecond pulse laser irradiation and also examines the recombination effects on energy transport from the microscopic viewpoint. In addition, the influence of laser fluence and pulse duration is studied by using the self-consistent three-temperature model, which involves carriers, longitudinal optical phonons, and acoustic phonons. It is found that a substantial non-equilibrium state exists between carriers and phonons during short pulse laser irradiation because of time scale difference between the relaxation time and the pulse duration. It is clear that the two-peak structure in carrier temperature exists and it depends mainly on laser pulses, fluences, and recombination processes. During laser irradiation, in particular, the Auger recombination for Si becomes dominant due to the increase in the carrier number density, whereas for GaAs, the Auger recombination process can be ignored due to an abrupt increase in SRH recombination rates at the initial stages of laser exposure. [doi:10.2320/matertrans.47.2835]

(Received May 22, 2006; Accepted September 22, 2006; Published November 15, 2006)

Keywords: *short pulse lasers, direct-band-gap, indirect-band-gap, silicon, gallium arsenide (GaAs), longitudinal optical (LO) phonons, acoustic phonons, carriers, nonequilibrium, SRH (Shockely-Read-Hall), Auger recombination*

1. Introduction

Even if conventional lasers, diamond saws, and water jets are used commercially as a variety of cutting and machining utilities, none of them can achieve the precision of the ultrafast pulse laser machine tool. The ultrashort pulse lasers being of pulsed shorter than typically 10 ps can generate easily very high optical peak power which is enough for full ionization of almost any solid matter,[1,2] and their non-equilibrium characteristics opened news and interesting possibilities in microfabrications, cellular nanobiosurgery technology, thin film characteristics measurement, environmental technology, and so on.[3] Nonequilibrium between electron-hole pairs (hereafter called carriers) in semiconductors and phonons is already significant on the picosecond time order, in which the carrier temperature can be much higher than the lattice temperature, and its energy transport have been very active research topics in the past two decades.

Energy transport during laser irradiation is explained by electron-hole excitation, photon-carrier-phonon interactions, and recombination processes, as seen in Fig. 1.[4] First, a valence electron excited by absorbing the photons results in an electron in the conduction band and a hole in the valence band. The carriers transfer their energies eventually into two different types of phonons being of optical and acoustic modes in the lattice. Because of higher energy levels compared to acoustic phonons, the optical phonons interact with electromagnetic waves more easily. It is clear that the group velocity of optical branch is close to zero or negligible compared to that of the acoustic branch. The optical phonons are also associated with an oscillating dipole that scatters radiation, and they scatter and emit acoustic phonons which are responsible for lattice heat conduction.

In general, the recombination process depends substantially on band structures as seen in Fig. 2, and it becomes very crucial in energy transport mechanism. It indicates the carrier loss owing to the process which the free electrons are captured by ionized donors and lose their energy in the nonradiative and radiative ways.[5] For indirect bandgap semiconductors as silicon, the conduction-band minimum and the valence-band maximum occur at different wave

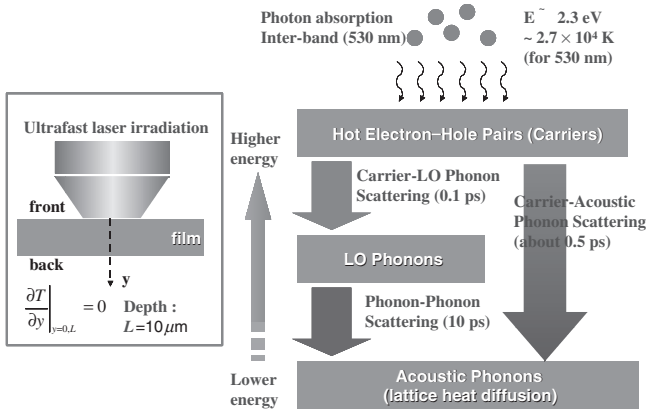

Fig. 1 Schematics of computational domain and mutual interactions among photons, LO phonons, and acoustic phonons.[4]

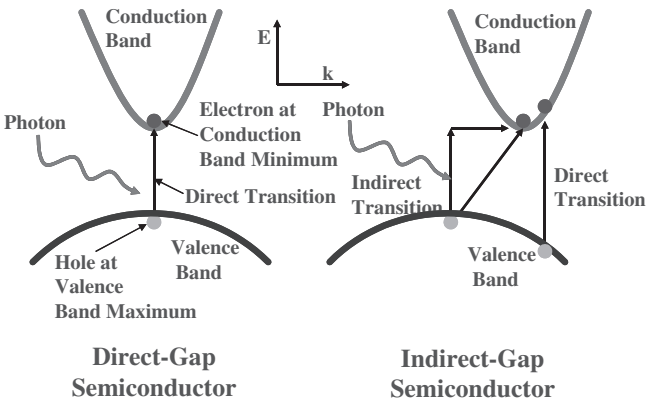

Fig. 2 Optical excitations in direct and indirect gap semiconductors.[1]

*Corresponding author, E-mail: shinyoun@cau.ac.kr

numbers, whereas for direct-band-gap semiconductors such as GaAs, GaSb, and InAs, they take place at the same value of wave number.[1,6,7] For silicon, Auger recombination is known to be a dominant process for very high carrier number density (typically, $N_C > 10^{18}\,\mathrm{cm}^{-3}$).[8] On the other hand, in direct-band-gap materials such as GaAs, GaSb, and InAs, three recombination processes are involved:[9] (1) Radiative recombination in which the excited electron and hole recombine and emit a photon, (2) Shockley-Read-Hall (SRH) nonradiative recombination or thermal recombination via the recombination center, in which the electron and the hole recombine and release a phonon to lattice, and (3) Auger recombination, where the extra energy released by the electron and hole recombination will be absorbed by another nearby electron or hole. Most researchers[8,10,11] simulated the carrier-phonon interaction for a single thermodynamic system where longitudinal optical (LO) phonons and acoustic phonons are in equilibrium state. This assumption is not valid because there is clearly nonequilibrium energy transport process between two phonons during very short but finite time scale. Hence, the present study establishes the three-temperature model and conducts the extensive simulation to investigate close interactions among carriers, LO phonons, and acoustic phonons for Si and GaAs film structures irradiated by subpicosecond pulse lasers. In particular, the role of recombination process on energy transport mechanism is discussed and the influence of laser fluence and pulse duration on nonequilibrium heat transfer is examined.

2. Governing Equations and Computational Details

The consistent numerical equations should be modeled to demonstrate the energy transport mechanism among carriers, LO phonons, and acoustic phonons. The carrier number density equation derived from the conservation equation is as follows:

$$\frac{\partial N_C}{\partial t} = \frac{\alpha_1 I}{h\nu} - \phi(N_C) + \delta(T_c)N_C, \tag{1}$$

$$I = \frac{0.939J(1-R)}{t_P}\exp\left(-\int_0^y \alpha_1 dz\right)\exp\left(-\frac{2.773t^2}{t_P^2}\right). \tag{2}$$

In eq. (1), the first term on the right side represents the absorption source that corresponds to direct transition that excites an electron to the conduction band and creates an electron-hole pair. The last term indicates the carrier generation due to impact ionization process. The second term means the recombination process associated with heating and destruction processes in carrier number density. The recombination process in semiconductors thin film structures differs according to the band-gap structures generally.[1,6,7] For indirect-band-gap materials, such as Si and Ge, Auger recombination process is dominant as follows:[4,8]

$$\phi(N_C) = \gamma N_C^3, \tag{3}$$

Unlike indirect-band-gap materials, in direct-band-gap materials such as GaAs, there are three well-known recombination mechanisms in $\phi(N_C)$.[9]

$$\phi(N_C) = \gamma_{sr}N_C + (\gamma_{rad} + \gamma_{SRH})N_C^2 + \gamma_{auger}N_C^3, \tag{4}$$

In eqs. (3) and (4), γ_{sr}, γ_{rad}, γ_{SRH}, and γ_{auger} denote the empirical coefficients via surface recombination, SRH recombination, and Auger recombination, respectively. For GaAs, at room temperature, the Auger process is not the dominant recombination mechanism in spite of high concentrations of electrons and holes. Auger recombination can be ignored because SRH recombination rates increase abruptly at the early time of laser irradiation. Since the size of laser beam is large compared to the laser penetration depth, the present equations can be modeled as one-dimensional. In most of previous work,[1,4] the lattice was assumed to be a single thermodynamic system which cannot be justified owing to differences between energy relaxation times between LO phonons and acoustic phonons. Hence, the present study establishes the three-temperature model including three energy conservation equations for carriers, LO phonons, and acoustic phonons as follows:[1,4]

$$\frac{\partial U_C}{\partial t} = \frac{\partial}{\partial y}\left(\kappa_C \frac{\partial T_C}{\partial y}\right) - \frac{3N_C k_B}{2\tau_{C-O}}(T_C - T_O) - \frac{3N_C k_B}{2\tau_{C-A}}(T_C - T_A) + \alpha_1 I, \tag{5}$$

$$\frac{\partial U_O}{\partial t} = \frac{3N_C k_B}{2}\left(\frac{T_C - T_O}{\tau_{C-O}}\right) - C_O\left(\frac{T_O - T_A}{\tau_{O-A}}\right), \tag{6}$$

$$\frac{\partial U_A}{\partial t} = \frac{\partial}{\partial y}\left(\kappa_A \frac{\partial T_A}{\partial y}\right) + \frac{3N_C k_B}{2}\left(\frac{T_C - T_A}{\tau_{C-A}}\right) + C_O\left(\frac{T_O - T_A}{\tau_{O-A}}\right), \tag{7}$$

where, $U_O = C_O T_O$, $U_A = C_A T_A$, and $U_C = C_C T_C + N_C E_g$ where E_g is the band-gap energy of material. In addition, τ_{C-O}, τ_{C-A}, and τ_{O-A} can be rigorously expressed in terms of temperature, laser frequency, carrier number density, and the other factors. In fact, the relaxation times are very difficult to be estimated rigorously. The present study thus assumes that constant relaxation times are used from the literature for simplicity of calculation.[12,13] Since LO phonons with negligible group velocity cannot contribute to lattice heat conduction, there is no heat diffusion term in the right-hand side of eq. (6). The important role of optical phonons is to provide the efficient intermediate path for heat transfer from source due to photon absorption to energy sink. This energy cascade depends mainly on relaxation times as well as heat capacities of carriers, LO phonons, and acoustic phonons. The physical properties of semiconductors taken from open literatures[1,5,6,9,12,14–21] are listed in Table 1.

The finite difference method with fully implicit scheme is used for discretizing the set of governing equations, and numerical accuracy is the second order for spatial and transient terms. The initial time was set to $t_{init} = -5t_p$ for all cases. Initially, the carrier and lattice temperatures are maintained at 300 K, and the initial carrier number densities are taken $1.18 \times 10^{10}\,\mathrm{cm}^{-3}$ for Si and $2.25 \times 10^{6}\,\mathrm{cm}^{-3}$ for GaAs.[5] As depicted in Fig. 1, the von Neumann boundary conditions with the zero gradient at $y = 0$ and $y = L$ are used for temperatures of carrier and two phonons on the basis of the assumption that during the short period of laser heating, heat losses from the front and back surfaces are likely neglected.[11] Finally, numerical solutions are obtained when the residuals from energy equations are less than 10^{-4}. For

Table 1 Physical properties of (a) Si and (b) GaAs.

(a) Silicon	
Properties	Expressions
C_C	$3N_Ck_B$.
C_A	$2.066\times10^6 - 9.91\times10^4(\theta_D/T_A)^{1.948}$, where $\theta_D \approx 645\,\mathrm{K}$ [6]
C_O	$2.49\times10^5 N_0 k_B\left(\frac{\theta_E}{T_O}\right)^2\frac{\exp(\theta_E/T_O)}{[\exp(\theta_E/T_O)-1]^2}$, where $\theta_E = h\nu/k_B \approx 731\,\mathrm{K}$ [6]
k_c	$-0.556 + 7.13\times10^{-3}T_C$ [21]
k_A	$1.585\times10^5/T_A^{1.23}$ [15]
τ	$\tau_{C-A} = \tau_0[1+(N_c/N_{c,cr})^2]$ where $\tau_0 = 0.5\,\mathrm{ps}$ and $N_{c,cr} = 2\times10^{27}$ [21]; $\tau_{C-O}\approx 0.1\,\mathrm{ps}$ [1] and $\tau_{O-A}\approx 10\,\mathrm{ps}$ [1]
α_1	$5.02\times10^5\exp(T_A/430)$ for $\lambda = 530\,\mathrm{nm}$ [17]
γ_{Auger}	3.8×10^{-43} [18]
R	$0.37 + 5\times10^{-5}(T_A - 300)$ for $\lambda = 530\,\mathrm{nm}$ [17]
E_g	$1.167 - 0.0258[T_A/300] - 0.0198[T_A/300]^2$ [14]

(b) Gallium arsenide	
Properties	Expressions
C_C	$3N_Ck_B$.
C_A	$9.17\times10^5 - 4.40\times10^4(\theta_D/T_A)^{1.948}$, where $\theta_D \approx 344\,\mathrm{K}$ [6,19]
C_O	$6.86\times10^{28}k_B\left(\frac{\theta_E}{T_O}\right)^2\frac{\exp(\theta_E/T_O)}{[\exp(\theta_E/T_O)-1]^2}$, where $\theta_E = h\nu/k_B \approx 429\,\mathrm{K}$ [6,19]
k_c	$k_B^2\sigma_C\frac{T_C}{q^2}\left[6F_2(\eta_c)F_0(\eta_c) - \frac{4F_1^2(\eta_c)}{F_0^2(\eta_c)}\right]$ [5]
k_A	$5.44\times10^4/T_A^{1.2}$ [14]
τ	$\tau_{C-A}\approx 0.5\,\mathrm{ps}$ [19] $\tau_{C-O}\approx 0.1\,\mathrm{ps}$ [12] $\tau_{O-A}\approx 10\,\mathrm{ps}$ [19]
γ_{rad}	$7.21\times10^{-16}\times(E_g/E_{g,ref})^2(T_A/300)^{-3/2}$ [6,20]
γ_{SRH}, γ_{Auger}	10^{-14} and 10^{-43}, respectively [6,20]
R	0.3–0.33 [14]
E_g	$1.519 - \frac{5.405\times10^{-4}T_A^2}{T_A+204}$ [9]

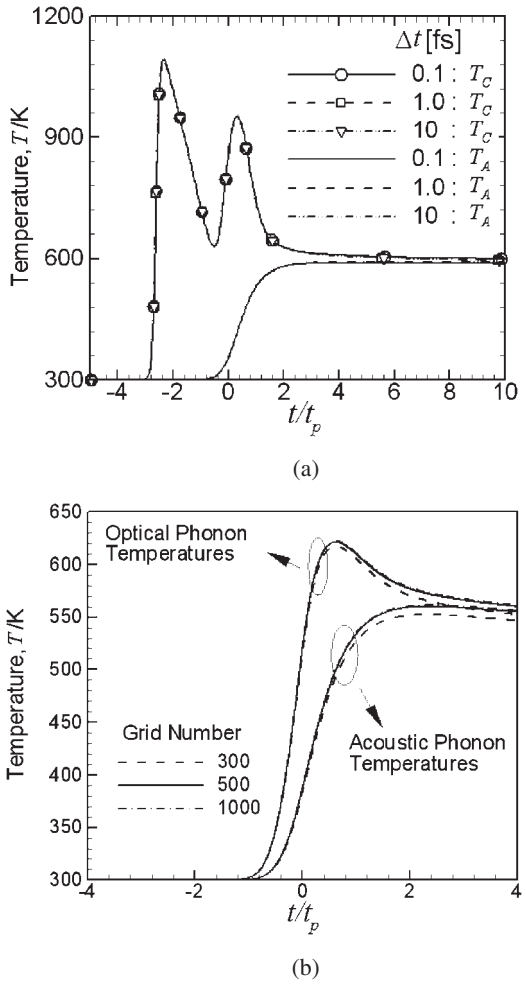

Fig. 3 (a) Influence of the time step on numerical estimation of different temperature (silicon) and (b) grid independence tests (silicon).

$\lambda = 530\,\mathrm{nm}$, all simulations are performed for a fixed film thickness of $10\,\mu\mathrm{m}$. Furthermore, the present study examines the sensitivities of time step and mesh size on the final solutions as seen in Fig. 3.

3. Results and Discussion

3.1 Thin silicon film structures (indirect-band-gap materials)

Figure 4 illustrates the time evolution of carrier, LO phonon, and acoustic phonon temperatures, and carrier number density for two different fluences when $\lambda = 530$ nm and $t_p = 10\,\mathrm{ps}$. The drastic increase in carrier temperature is observed for pulse lasers of a few picosecond duration, whereas the temperature rise of acoustic and LO phonons is relatively small. A substantial nonequilibrium occurs mainly due to the scale difference between energy relaxation time and laser pulse duration. In particular, it is interesting to note the existence of two-peak structure in the carrier temperature because both the laser pulse and rapid Auger recombination heat the plasma and dominate as plasma heat sources at different times during the pulse.[8,11] It suggests that thermal nonequilibrium state are likely able to be controlled by laser fluence as well as pulse duration time. The carrier temperature again rises near $t = 0$, at which the carrier number density increases substantially and Auger recombination converts carrier ionization energy into kinetic energy at a sufficiently large rate to again cause the carrier temperature to increase.[8] From Fig. 4(b), the carrier number density increases during laser irradiation and its peak increases with the increase of laser fluence. As the laser intensity increases, the Auger recombination becomes important during irradiation because this type of recombination becomes dominant at high carrier concentrations in silicon.[5] Once the carrier number density decreases, the carrier temperature begins falling but nonequilibrium between carriers and lattice phonons maintains for long times because of on-going Auger recombination.[11] As time goes, however, all energies are in equilibrium state as seen in Fig. 4(a). The maximum carrier temperatures for 50 and $150\,\mathrm{mJ/cm^2}$ are estimated about 1000 K, which corresponds to about 86 meV which is much smaller than incident photon energy of about 2.3 eV for $\lambda = 530\,\mathrm{nm}$, whereas equilibrium temperatures are observed at 390 and 600 K for $J = 50$ and $150\,\mathrm{mJ/cm^2}$, respectively. At the early stage of laser exposure, the carrier energy increases considerably due to carrier heat capacity much

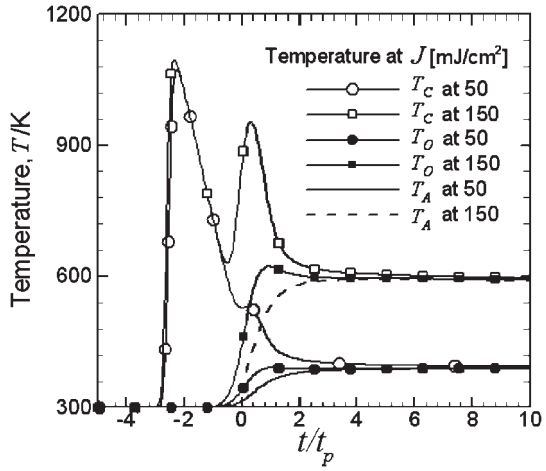

(a)

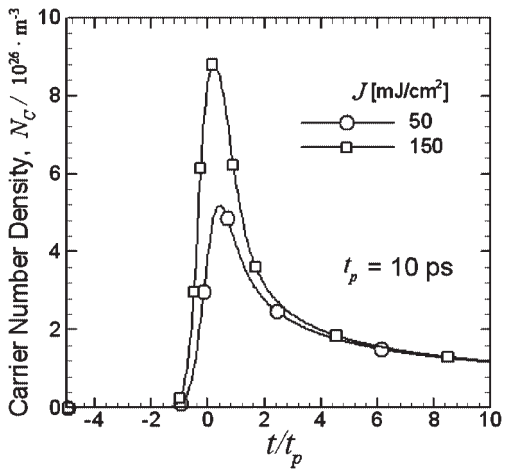

(b)

Fig. 4 (a) The temperature estimation of carriers, LO phonons, acoustic phonons and (b) transient behaviors of carrier number densities for 50 and 150 mJ/cm^2 at $t_p = 10$ ps (silicon).

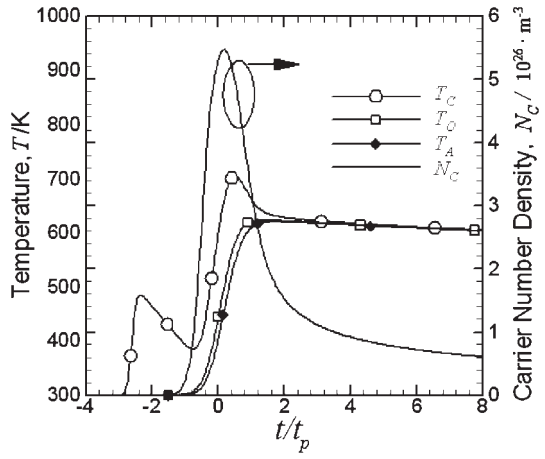

(a) 50 ps

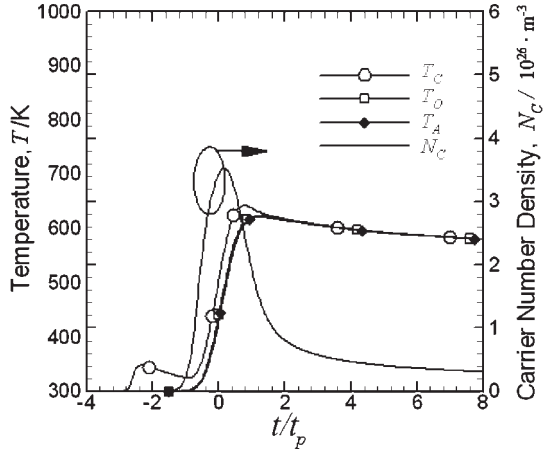

(b) 200 ns

Fig. 5 Estimation of carrier, LO phonon, acoustic phonon temperatures, and carrier number densities at 150 mJ/cm^2 for different laser pulses (silicon).

smaller than those of two phonons. After the finite time, they lose energy to the phonons through emission of LO phonons, and the temperature difference between carriers and LO phonons makes it possible to transfer energies to acoustic phonons which are responsible for heat conduction. From Fig. 4(a), the time when LO phonon temperature begins to increase is slightly faster than that when acoustic phonon does. This time lag is because of a finite scattering rate between two phonons.

It turns out from Fig. 5 that the peak values of carrier temperature decreases with the increase of pulse duration. It leads to the drastic reduction of carrier number density and the extent of nonequilibrium decreases as pulse duration increases. The carriers, LO phonons, and acoustic phonons are in nearly thermal equilibrium. It is because the laser pulse is much longer than the relaxation times for carrier-phonon and phonon-phonon scatterings. Also, it is observed from Figs. 4 and 5 that the laser pulse hardly affects the increase in lattice temperature, relative to the laser intensity. Besides, the carrier number density increases with laser fluence and its decaying rate increases because of the Auger recombination.

3.2 Thin gallium arsenide (GaAs) film structures (direct-band-gap materials)

Figure 6 illustrates *in-situ* estimations of carrier temperatures and two different phonon temperatures at the film surface with respect to time normalized by the pulse duration. The carrier temperature increases rapidly com pared to the temperatures of LO phonons and acoustic phonons. Similar to the case of silicon, it is found that a substantial nonequilibrium among carriers and two phonons takes place due to the scale difference between energy relaxation times and laser pulse durations, and a two-peak structure in carrier temperature exhibits during laser exposure. The first peak occurs in the early stage of laser exposure because carrier heat capacity is several orders of magnitude smaller than phonon heat capacities (regime 1). The second peak appears clearly because of non-radiative recombination process that heats the plasma (regime 2). As like the case of silicon, it also confirms that the assumption of single thermodynamic system is no longer valid for ultra-short pulse laser heating problems. Compared to the silicon case, however, somewhat different tendencies can be found in carrier temperature. It suggests that the first peak value is higher than the second peak value for silicon, whereas the

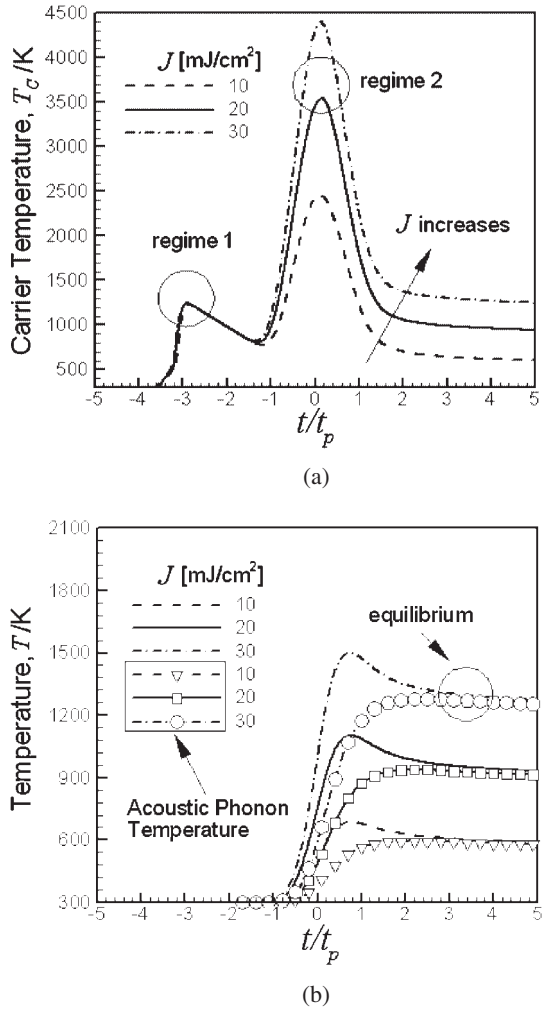

Fig. 6 Estimation of (a) carrier temperature and (b) two different phonon temperatures for various laser fluences at $t_p = 10\,\text{ps}$ (GaAs).

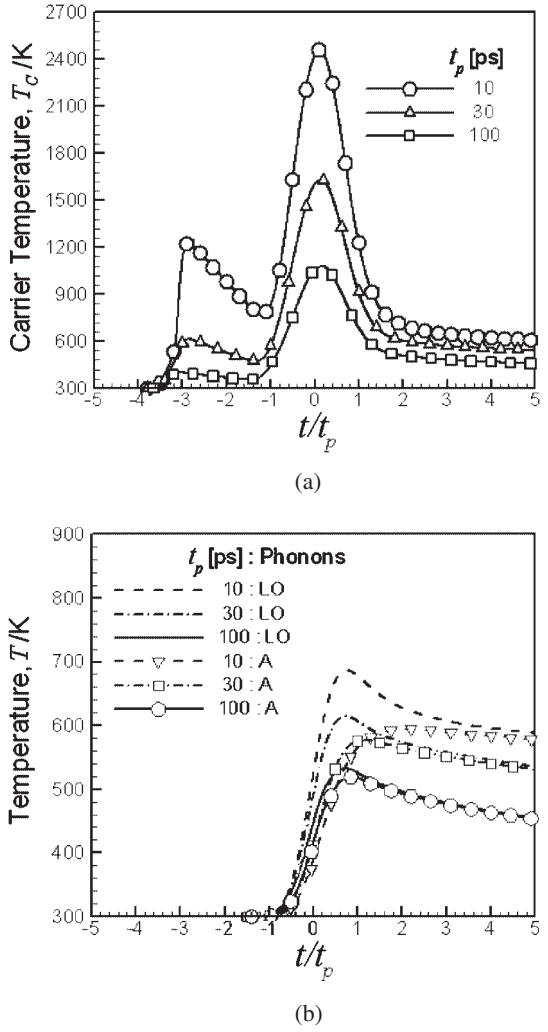

Fig. 7 Influence of pulse duration on (a) carrier temperatures and (b) two different phonon temperatures at $J = 10\,\text{mJ/cm}^2$ (GaAs).

second peak of carrier temperature is rather higher than the first peak value for GaAs. This is because of different recombination processes that significantly affect the carrier number densities. Figure 7 represents the pulse duration effects on temperatures, and shows the peak value of carrier temperature increases with the decrease of laser pulse duration. As explained previously, the nonequilibrium state exists obviously between LO phonons and acoustics phonons when the laser pulse is relatively short, whereas when $t_p = 100\,\text{ps}$, two phonon temperatures are nearly in equilibrium state owing to pulse duration much longer than relaxation times. There is also such a time lag similar to the silicon case, indicating that the time at which LO phonon temperature starts to increase is slightly faster than that when acoustic phonon does. For the pulse duration longer than energy relaxation time, the time lag will disappear due to thermal equilibrium state between two phonons. In GaAs or other III-V materials unlike silicon, even stronger coupling to electron-hole pairs is present due to the polar interactions and it makes LO phonons emitted more efficiently. Because LO phonon energies are higher than those of acoustic phonons, LO phonon emission is a faster and more efficient way to transfer energy. Figure 8 represents the spatial temperature distributions of LO and acoustic phonons at $t = 0\,\text{ps}$ when laser energy peaks. The maximum diffusion depth is estimated about 0.5 μm when all temperatures are in equilibrium. It is clearly observed that as laser pulse increases, temperature difference between two phonons decreases. It means that two phonons are in equilibrium state.

The recombination processes, each of which affects carrier number density and temperatures in GaAs structures, are very important for better understanding of energy transfer in semiconductors. For this reason, the present study deals with four different cases for the given conditions such as $J = 10\,\text{mJ/cm}^2$ and $t_p = 10\,\text{ps}$: Case 1 indicates that all recombination processes are included. For case 2, Auger recombination is solely considered. Case 3 includes Auger recombination and SRH recombination. Case 4 discusses the effect of Auger recombination and radiative recombination. From the comparison, it is seen in Fig. 9(a) that cases 1 and 3 show similar tendency but cases 2 and 4 represent quite different patterns near the regime 2 where recombination becomes dominant. For cases 2 and 4, the estimation of lower carrier temperature near the regime 2 results from under-prediction of the decrease in carrier number density due to the recombination. It is found from Fig. 9(b) that the SRH recombination, one of non-radiative recombination process-

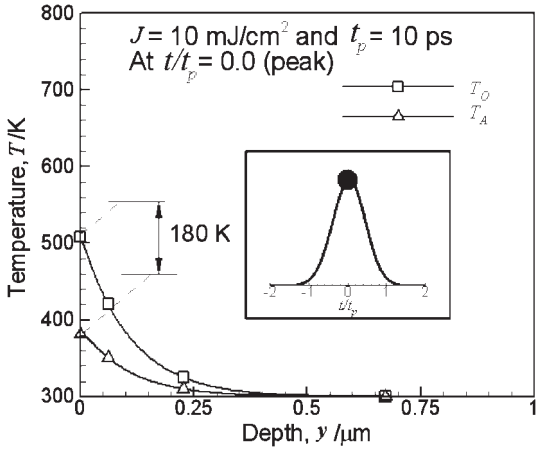

(a)

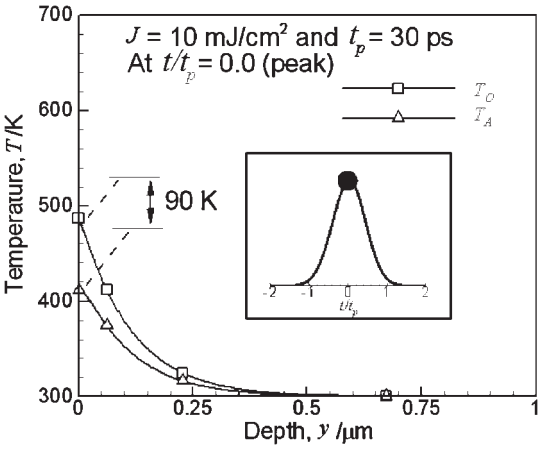

(b)

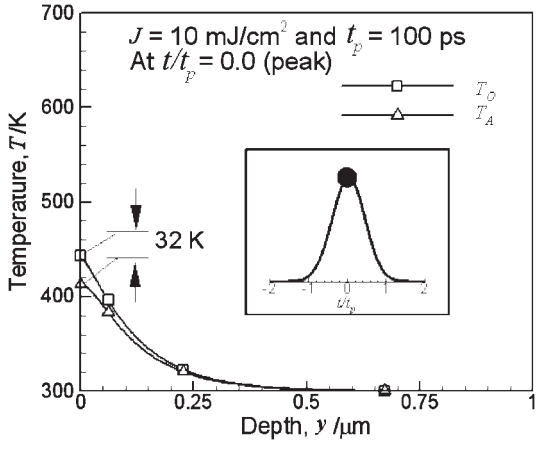

(c)

Fig. 8 The spatial distribution of LO and acoustic phonon temperatures for various pulse widths at $t = 0$ when laser energy peaks.

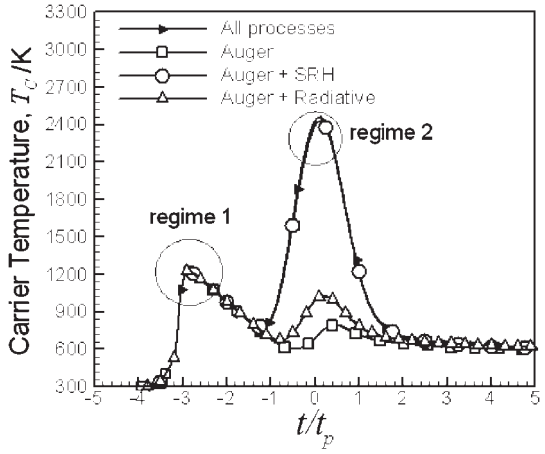

(a)

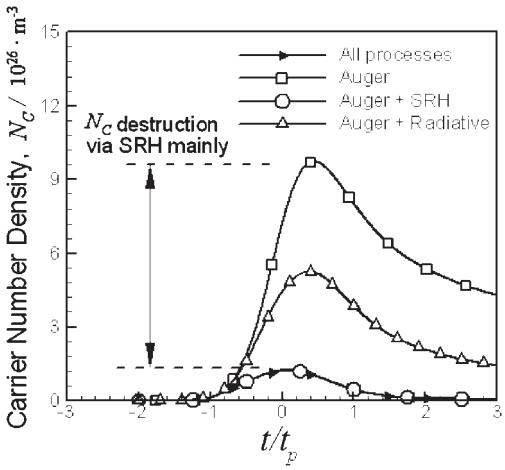

(b)

Fig. 9 Time evolution of (a) carrier temperature and (b) carrier number density for different cases (GaAs).

es, plays an important role in decreasing carrier number density. According to previous works,[5,11] Auger recombination is activated more vigorously when the carrier number density is very high, whereas the SRH recombination rate in GaAs event at room temperature is quite high compared to Auger recombination rate. Meyer and his colleagues suggested that as temperature increases, Auger recombination becomes dominant as in the other materials.[14] However, their suggestion would not be justified for short pulse laser heating in GaAs materials.

Figure 10 represents various recombination rates during laser irradiation and supports the aforementioned discussion on carrier number density. The SRH recombination rates have already increased sufficiently compared to other recombination rates near the initial stage of laser exposure. In general, the Auger recombination becomes dominant in destructing carriers for very high carrier number density.[5] Unfortunately, in GaAs materials, the SRH recombination contributes to destruct energy carriers at the early stage of laser exposure, leading that the Auger recombination rate is no longer augmented. Besides, even radiative recombination rate is somewhat higher than Auger recombination rate. It is found that the SRH recombination becomes important and it should be considered for direct-band-gap materials, whereas Auger recombination can be neglected even at high temperature. This fact is likely consistent with the conclusion of Zhang and his colleagues.[22]

4. Conclusions

This article reports numerically the micro heat transfer

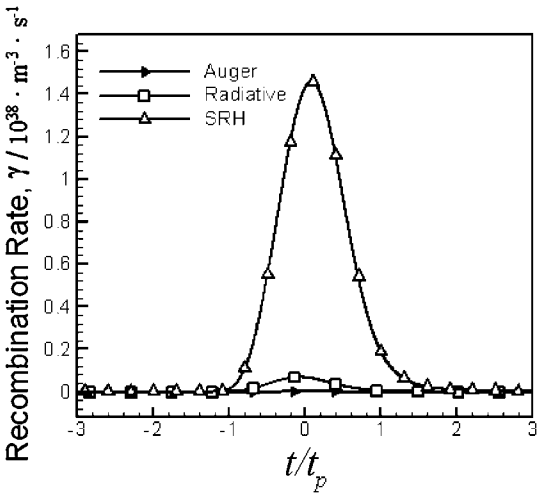

Fig. 10 Estimation of recombination rates with respect to normalized time (GaAs).

characteristics in thin Si and GaAs film structures heated by the subpicosecond pulse laser through the three-temperature model. The role of recombination processes on energy transfer is discussed, and the influence of laser fluence and pulse duration are also studied for different types of semiconductor materials. The following conclusions can be drawn.

(1) It is confirmed that the nonequilibrium among carriers, LO phonons, and acoustics phonons exhibits during a finite time after which all of them are gradually equilibrated as time goes. A two-peak structure in carrier temperature can be found, and it occurs due to the recombination and the difference of heat capacities. The peak values of carrier temperature decreases with the increase of pulse duration, resulting in drastic reduction of carrier number density. In addition, the laser pulse hardly affects the increase in lattice temperature, relative to the laser intensity.

(2) For longer pulses, this lagging effect eventually disappears. In this case, a single thermodynamic system assumption is justified. But, for short pulse laser heating, the three-temperature model is suitable for simulating nonequilibrium between LO phonons and acoustic phonons within a finite time lag.

(3) For indirect-band-gap materials like silicon, the Auger recombination is a dominant process on carrier number density. However, in direct-band-gap materials such as GaAs, the Auger recombination is negligible relative to other recombination processes. It is found that the SRH recombination, one of non-radiative recombination processes, plays an important role in decreasing carrier number density, and it is quite high compared to the Auger recombination rate.

Acknowledgements

This work was supported by grant No. (R01-2004-000-10572-0) from the Basic Research Program of the Korea Science & Engineering Foundation.

REFERENCES

1) C. L. Tien, A. Majumdar and F. M. Gerner: *Micro-scale Energy Transport* (Taylor & Francis, Washington D.C., 1998).
2) L. M. Phinney and C. L. Tien: ASME Journal of Heat Transfer **120** (1998) 765–771.
3) J. D. Chlipala, L. M. Scarforne and C. Y. Lu: IEEE Transaction of Electronic Devices **36** (1989) 2433–2439.
4) S. H. Lee: Journal of Mechanical Science and Technology **19** (2005) 1427–1438.
5) R. F. Pierret: *Advanced Semiconductor Fundamentals, Modular Series on Solid State Device*, Vol. 6 (Addison-Wesley Publishing Company, 1983)
6) C. Kittel: *Introduction to Solid State Physics*, 6th edition (Wiley, New York, 1986).
7) G. Chen: *Nanoscale Enegy Transport and Conversion, a Parallel Treatment of Electrons, Molecules, Phonons, and Photons* (Oxford University Press, 2004).
8) H. M. van Driel: Physical Review B **35** (1987) 8166–8176.
9) G. P. Agrawal and N. K. Dutta: *Semiconductor Lasers* (Wan Nostrand Reinhold, NY., 1993).
10) T. Q. Qiu and C. L. Tien: International Journal of Heat and Mass Transfer **37** (1994) 2789–2797.
11) S. H. Lee, J. S. Lee, S. Park and Y. K. Choi: Numerical Heat Transfer, Part A **44** (2003) 833–850.
12) C. L. Collins and P. Y. Yu: Phys. Rev. B **30** (1984) 4501–4515.
13) P. Lugli, P. Bordone, L. Reggiani, M. Rieger, P. Kocevar and S. M. Goodnick: Phys. Rev. Lett. **39** (1989) 7852–7865.
14) J. R. Meyer, M. R. Kruer and F. J. Bartoli: Journal of Applied Physics **51** (1980) 5513–5522.
15) R. F. Wood and G. E. Giles: Phys. Rev. B **23** (1981) 2923–2942.
16) A. Raman, D. G. Walker and T. S. Fisher: Solid-State Electronics **47** (2003) 1265–1273.
17) G. E. Jellison and F. A. Modine: Phys. Rev. B **27** (1983) 7466–7472.
18) J. Dziewior and W. Schmid: Appl. Phys. Lett. **31** (1977) 346–348.
19) A. Majumdar, K. Fushinobu and K. Hijikata: ASME Journal of Heat Transfer **117** (1995) 25–31.
20) K. Seeger: *Semiconductor Physics*: An Introduction, 5th edition (Springer, New York, 1991).
21) D. Agassi: J. Appl. Phys. **55** (1984) 4376–4383.
22) X. Zhang, J. Wen and C. Sun: Appl. Phys. A **76** (2002) 261–267.